

# Study of the Distribution and Shape of the Pores in Silica Porcelain

MARIA GOREA\*, FERENC KRISTALY

Babes-Bolyai University, 1 M. Kogalniceanu Str., Cluj Napoca, 400084, Cluj, Romania

*Two industrial chemically-similar compositions of electric silica porcelain, containing variable amounts of kaolin, feldspar and quartz, have been tested for their microstructure. The crystalline and glassy phases, and the pores in the studied samples were investigated by optical and electron microscopy. The number of measured pores in identical area sections in the two samples differs in relationship with the type and amount of raw materials used. Sample R4, with a higher concentration of clay minerals and a lower quartz amount presented twice as many closed, larger pores as sample R3, which was obtained from higher amounts of feldspar and lower clayey materials. On the contrary, the roundness of pores in sample R4 is higher than that of pores in sample R3. SEM pictures of the investigated ceramic surfaces illustrate the study.*

*Keywords: silica porcelain, microstructure, pores*

Porcelain is one of the oldest materials used as electric insulator due to some of its properties, *i.e.*: mechanical strength, high-power dielectric strength and corrosion resistance. The most frequently used porcelain insulators are rich in silica or alumina, being classified as groups C-110 and C-120 according to the IEC 6672-3 standard.

The silica porcelain consists of a vitreous phase (matrix) and some dispersed/embedded crystalline phases. The dominant crystalline phases are represented by mullite and quartz, sometimes cristobalite, the crystals having various sizes according to the type and amount of raw materials and to the thermal treatment applied.

The porcelain's electric and mechanical characteristics depend on both the properties of the crystalline phases (crystal size and distribution, some isomorphous substitutions in the crystalline network), and those of the vitreous phase (presence of some ions, especially Na<sup>+</sup> and K<sup>+</sup> from the feldspar melt) and of the pores (shape, size, distribution). It was shown that porcelain strength decreases with the increase of the amount, size and asymmetric size distribution of mullite crystals, but increases with the increase of quartz, cristobalite and vitreous phase [1].

The characterization and identification of mineral phases and the presence of amorphous one in X-ray patterns, the dependency of mechanical properties of silica- and alumina-rich porcelain on the original composition and the thermal treatment was long time ago emphasized, but it is still an actual research topic [2,3]. The large quartz grains unevenly distributed in the glassy matrix cause the occurrence of micro cracks, thus contribute to the strength decrease of the silica porcelain. Higher homogeneity of quartz crystals size distribution and average sizes between 10-20 μm limit the negative effects due to the occurrence of fissures in the matrix [4].

The microstructure of standard silica porcelain consists of α quartz and mullite crystals in a glassy matrix, while alumina-rich porcelain also contains corundum. The mullite crystals growth from the clay minerals-feldspar interface on feldspar relics was observed, indicating the transformation of primary mullite into secondary mullite [5, 6]. At optimum firing temperature for each raw materials mixture (receipt), the amount of melt has to provide the

crystalline phases and to react with them in a corresponding time interval according to the firing diagram. A lower firing temperature determines the formation of open pores in the ceramic body, while a higher temperature leads to increasing porosity, especially amount of closed pores, as a result of oxygen release during Fe<sub>2</sub>O<sub>3</sub> decomposition and gas expansion in the pores [7].

The aim of this paper is to characterize the pores from the glassy matrix of two silica electric porcelain types, of different compositions. The pores size, shape and distribution, and their correlation with the chemical composition of the glassy phase are investigated.

## Experimental part

The tested materials are two masses of silica porcelain of different compositions (R3 and R4) obtained industrially for being used as ceramic components of low voltage electrical devices. Compositionally, the concentration of clay raw materials is 43 % in the R3 ceramic mass and 47.5 % in the R4; the feldspar (F) to sand (N) ratio is 1.28 (corresponding to an F/N ratio of 32:25 for R3, and 29.5:23 for R4). The characteristics of the raw materials and the correlation with the microstructure of the corresponding ceramics were presented in a previous publication [8].

The processing of the raw materials mixture was performed by wet grinding in a ball mill. The slurry was dried by pulverisation at about 7 % humidity and the powder was then semidried pressed in metal dies. The pressed and dried samples were submitted to thermal treatment at 1300°C for 10 h.

The bulk chemical composition of the R3 and R4 silica porcelain samples was determined by the industrial producer by following the standardized wet procedure.

For defining the chemical composition of the vitreous matrix in the two samples, energy dispersive measurements (EDX) were performed at the Department of Mineralogy and Petrology, University of Miskolc on a JEOL JXA-8600 Superprobe micro-beam electron microscope (acceleration voltage 15 kV, probe current 12 nA, beam diameter 10 μm, live time 90 s). It must be emphasized that during the measurements, the crystals - mainly mullite and quartz, visible at the electron microscope resolution were avoided. For each sample two by two measurement

\* email: mgorea@chem.ubbcluj.ro

lines were set up throughout the surface, representing “a” (two lines close to each other) and “b” sections (two lines). In the analysis small amounts of Mg, Ti, and P were ignored, due to insignificant presence of these elements.

The pores in the ceramic body were analysed in polished sections by digital image processing techniques: BSE images were processed using Image Tool 3 software package (fig. 1), to obtain the pore size ( $\mu\text{m}^2$ ) and pore roundness  $((4 \times \text{PI} \times \text{area}) / \text{perimeter}^2)$  patterns. The roundness of pores is dimensionless, perfect roundness equals 0.

## Results and discussions

According to the bulk chemical composition, as presented in table 1, samples R3 and R4 are relatively similar, at least concerning the concentration in main refractory oxides ( $\text{SiO}_2$ ,  $\text{Al}_2\text{O}_3$ ), and of flux alkaline ones ( $\text{Na}_2\text{O}$ ,  $\text{K}_2\text{O}$ ). A higher content of  $\text{Fe}_2\text{O}_3$  is present in sample R4 (twice as much as in R3) but the value is within the standards.

The main goal of the present study being the investigation of the shape and distribution of the closed pores in the vitreous matrix of ceramic samples (fig. 1), the vitreous matrix was also investigated from a chemical point of view.

The corresponding average oxide values and the standard deviation are presented in table 2.

Differences can be noticed concerning the various oxides present in the glassy phase, as well as variation of the same oxide in different investigated areas. It is worth to mention that  $\text{SiO}_2$  has lower contents in the matrix of sample R3 - 54.71 %, as compared to 60.98 % in R4, in spite of higher concentration of quartz in the bulk sample R3. In both samples, the  $\text{SiO}_2$  content is lower than that reported by other authors; for example, the comparative study [5] of a standard porcelain and an alumina-rich one, revealed higher silica contents (>80 %) both at the border of  $\alpha$  quartz, and in the quartz-lacking areas of the standard porcelain. Even in the alumina-rich porcelain the glassy phase was silica-rich, this fact being explained by the authors as a consequence of mullite formation from melts at temperatures above 1200°C. On the contrary, the  $\text{Al}_2\text{O}_3$  content is relatively high in both R3 and R4 samples. We assume that this feature could be correlated with the presence within the vitreous phase of very fine microcrystalline mullite that is beyond the SEM detection limit, but that can be quantified by EDX.

The contents of alkaline and earth-alkaline oxides do not show considerable variation in R3 as compared to R4. The values are relatively low (3-4 %  $\text{Na}_2\text{O} + \text{K}_2\text{O}$ ) as compared to reference data for standard porcelain (about 7 %  $\text{K}_2\text{O}$ ).

The microstructure of the two samples of silica porcelain was investigated by the means of optical microscopy under polarised light (POM) and scanning electron microscopy (SEM) (figs. 2 and 3). The optical microscopy images (fig. 2) evidence a large amount of crystalline phases, mainly represented by quartz in both samples, the secondary mullite crystals being less visible. The glassy-crypto-

crystalline phase is also present in large amounts, but it does not fill completely the pores of various sizes distributed within the whole surface of the samples.

The values for closed porosity, and shape and distribution of pores in the thermally treated silica porcelain are basically determined by the composition of the raw materials mixture and by the temperature-induced transformations. The clay minerals and the accompanying phases undergo a series of physical and chemical mass loss-involving processes during thermal treatment, such as dehydroxylation and dissociation, which influence porosity. Large sized elongated pores are the result of defective pressing procedures and thus they were not considered for data processing and interpretation. Figure 3 presents the areas from samples R3 and R4 submitted to the analysis of pores distribution, size and shape by electron microscopy.

The images R3a and R3b, and respectively R4a and R4b represent two different sections through the same sample; the investigation procedure evidenced both the internal (within each sample) variation of porosity (in sections “a” vs. “b”), and the inter-sample variation (R3 vs. R4). The spots selected for microchemical investigation, by EDX, belong to the same sections; the spots are located at 32  $\mu\text{m}$  distance, along the directions indicated in figure 3.

The number of pores measured in each investigated section is given in table 3. During image processing procedure, the pores have been identified as “objects” within the samples, the area of each investigated section being  $1.16 \times 10^6 \mu\text{m}^2$ . The pores have been classified according to their area ( $\mu\text{m}^2$ ) and roundness degree (dimensionless), parameters calculated by digital processing of the images. The closed porosity (% approximate values) was calculated by dividing the area of the measured pores ( $A_p$ ) with the total area of the section ( $A_t$ ), according to the formula:  $A_p / A_t \times 100$  (table 3).

The sections investigate in sample R3 show a remarkable lower number of pores as compared to sample R4, with less significant differences between sections “a” and “b” of the same sample. The difference between the calculated closed porosity in the two samples are mainly due to the variable pore counts in the investigated sections, while the differences between the samples are caused by the differences in ceramic masses compositions.

### Pore distribution according to the calculated area

The pores classification and distribution according to the calculated area was done based on selected size intervals for which the pore count was performed. The results are presented in table 4. The pores only partly located in the investigated section (image) were not taken into account, for example the elongated pores. In sample R3, there are remarkable differences concerning the distribution of small pores (30 - 100  $\mu\text{m}^2$ ), while the large size classes do not show notable differences. In sample R4, the two investigated sections are more similar, suggesting a more homogeneous sample. However, sample R4 shows a significant increase of both the amount

**Table 1**  
BULK CHEMICAL COMPOSITION OF THE ANALYSED SAMPLES

Sample/Oxide	$\text{SiO}_2$	$\text{Fe}_2\text{O}_3$	$\text{Al}_2\text{O}_3$	$\text{CaO}$	$\text{MgO}$	$\text{Na}_2\text{O}$	$\text{K}_2\text{O}$	Total
R3	73.86	0.32	21.12	0.63	0.55	1.82	1.70	100
R4	73.46	0.61	21.24	0.68	0.60	1.70	1.70	99.99

Sample/oxides		SiO <sub>2</sub>	Al <sub>2</sub> O <sub>3</sub>	CaO	Na <sub>2</sub> O	K <sub>2</sub> O	FeO
R3	Average	54.71	40.31	0.79	1.18	2.08	1.07
	Standard deviation	7.13	7.75	0.31	0.35	0.56	0.38
R4	Average	60.98	32.78	1.30	1.34	2.60	1.55
	Standard deviation	6.19	7.10	0.59	0.58	0.55	0.31

**Table 2**  
CHEMICAL COMPOSITION OF THE MATRIX  
OF THE SAMPLES

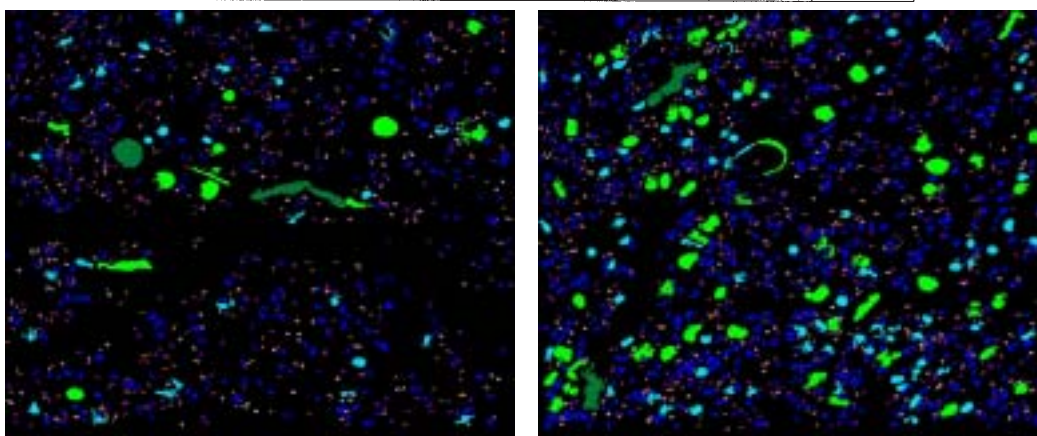


Fig. 1. BSE image of pores distribution into the ceramic sample: composition of R3 (left); composition of R4 (right)

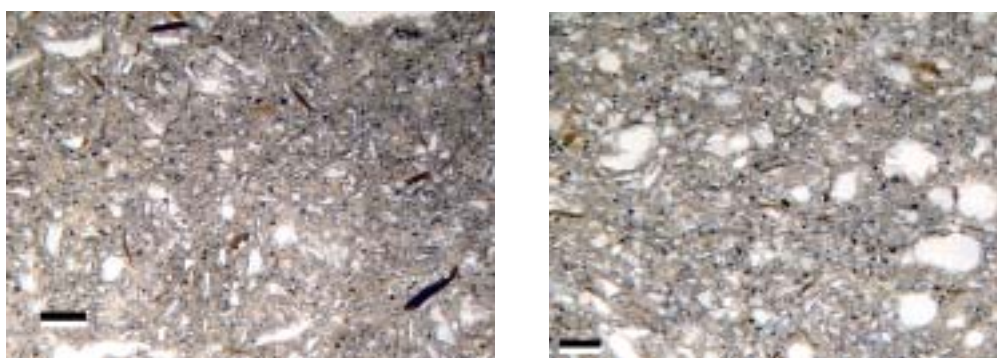


Fig. 2 Image of optical microscopy for silica porcelain: Sample R3 (left); sample R4 (right); 1N, 0,125mm bar.

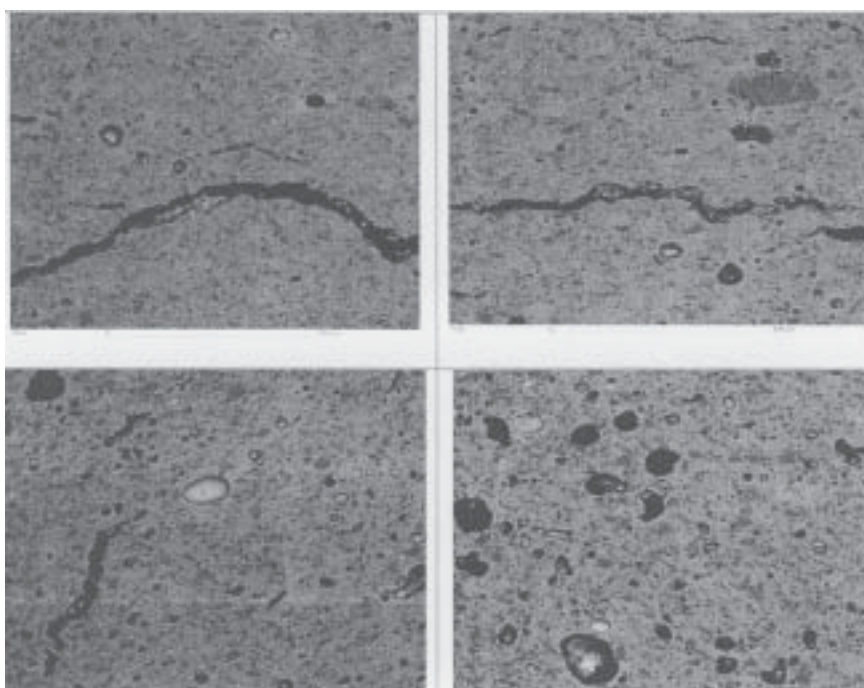


Fig. 3. Electronic microscopy SEM of analysed samples. Large pores haven't been taken into consideration at digital processing of images

**Table 3**  
THE NUMBER OF MEASURED PORES (1), THEIR CONCENTRATION (RATIO BETWEEN NUMBER OF PORES AND INVESTIGATED AREA) (2) AND THE CLOSED POROSITY (3)

	(1) Total counts (objects=closed pores)		(2) Nr. of objects/area		(3) $A_p/A_t \cdot 100$ (~closed porosity) (%)	
	a	b	a	b	a	b
R3	1010	1109	0.41	0.45	14.29	17.58
R4	1566	1432	0.63	0.58	29.48	33.98

**Table 4**  
SIZE DISTRIBUTION AND ROUNDNESS DEGREE OF THE INVESTIGATED PORES

	Area ( $\mu\text{m}^2$ )	Counts				Mean Value			
	Value Range	R3a	R3b	R4a	R4b	R3a	R3b	R4a	R4b
1	-30	0	0	0	0	0,00	0,00	0,00	0,00
2	30.00 - 50.00	170	198	191	227	45,65	45,72	45,38	45,39
3	50.00 - 70.00	258	332	324	326	58.94	58.99	58.40	58.63
4	70.00 - 100.00	204	175	251	255	83.81	82.92	82.80	83.39
5	100.00 - 500.00	334	356	664	512	192.87	195.51	203.54	213.92
6	500.00 - 1000.00	30	31	78	59	684.75	720.03	675.46	684.77
7	1000.00 - 3000.00	12	10	56	41	2263.14	1359.60	1583.20	1876.57
8	3000.00 -10000.00	2	5	2	9	7330.12	6505.72	6627.30	6770.35
9	10000.00 -	0	2	0	3	0.00	11214.14	0.00	15817.09
Roundness (adimensional)									
	Roundness	Count				Mean Value (Standard deviation)			
	Value Range	R3a	R3b	R4a	R4b	R3a	R3b	R4a	R4b
1	-0.06	8	7	6	15	0.05	0.04	0.06	0.05
2	0.06 - 0.10	21	15	71	51	0.09	0.08	0.09	0.08
3	0.10 - 0.30	470	207	886	790	0.20	0.21	0.20	0.20
4	0.30 - 0.50	315	452	390	390	0.39	0.40	0.39	0.39
5	0.50 - 0.60	119	247	129	108	0.55	0.55	0.54	0.54
6	0.60 - 0.80	70	125	82	75	0.66	0.66	0.66	0.67
7	0.80 -	6	57	2	3	0.83	0.87	0.82	0.82

of pores, as well as of relatively larger ones (interval no. 5 in table 4).

In the first three size classes, R4 shows about 20-25 % more pores as compared to sample R3; a progressive increase, from 35 % to 49 %, 71% and 78 % is noticeable for

the large size intervals. Even if elongated pores are not present in sample R4, as compared to R3, the amount of large pores is significantly higher in the former one, correlated to the higher concentration (additional 4.5 %)

of clay minerals in the bulk composition leading to twice as much closed porosity values in the ceramic product.

An explanation for this fact is given in reference [8], where the study of thermal behaviour of clayey raw materials has evidenced a significant mass loss until reaching 1000°C due to the presence of illite/montmorillonite in the kaolin-rich raw material.

The size-based classification of pores in the investigated sections indicates a symmetric, bimodal distribution with a slight deviation towards size interval no. 5 (100-500  $\mu\text{m}^2$ ).

In samples R4, the pore sizes are shifted to higher values; the size distribution curve is also bimodal, but the number of pores measured on the same area in both samples is higher.

The size of the pores is also influenced by the presence and amount of melt at firing temperature, lower amounts of flux providing smaller concentrations of melted phase. Table 4 illustrates the pores shape in samples R3 and R4, as values of roundness degree, i.e. the deviation from the ideal sphere (ideal sphere has 0 roundness degree).

As it was already shown, sample R4 contains more pores but with rounder shapes. Most of the pores show roundness values of 0.06 to 0.5. In comparison, sample R3 contains a significantly higher number of pores (a total of 258 as compared to 162 in sample R4), with roundness values above 0.5.

The relatively higher amount of melt in porcelain induces a higher contraction of the samples and higher sphericity deviation values of the rounded pores resulted from the decomposition of the raw materials.

## Conclusions

The microstructure of silica porcelain for low voltage electric insulators refers to crystalline phases – quartz and mullite, in a silica-alumina rich vitreous matrix that contains pores of various shapes and sizes.

The chemical composition of the vitreous phase in the investigated samples points to various Si and Al oxides contents, the  $\text{Al}_2\text{O}_3$  concentration being higher than the regular one reported for standard porcelain in the references. The composition of the vitreous phase may not

be possible to be investigated in detail, mainly because of the assumed presence of fine mullite microcrystals in the matrix below the resolution of the SEM, but evidenced by the EDX.

The pores present in the glassy matrix, resulting from the transformation of some minerals from the raw materials during thermal treatment show various sizes and shapes.

In the sample richer in clayey raw material and scarcer in feldspar (R4), a higher number of pores, larger in size has been evidenced. These pores have better roundness degrees, and the closed porosity has values twice as much than the other sample. A decrease with 2.5 % of the amount of feldspar and an increase with 4.5 % of the clay minerals content implies a double-as much value for the closed porosity, while the values for the open porosity are practically constant.

A basically bimodal size distribution of the pores was noticed in both investigated samples; only the pore counts per measured area represents a variable parameter. More rounded pores of larger sizes are present in sample R4, due to relatively lower amounts of melt.

## References

1. CHAUNDHURI, S.P., SARKAR, P., CHAKRABORTY, A.K., *Ceramics International*, **25**, 1999, p. 91
2. AMIGO, M. J., CLAUSELL, V.J., ESTEVE, V., DELGADO, M.J., REVENTOS, M.M., OCHANDO, E.L., DEBAERDEMAEKER, T., MARTI, F., *Journal of the European Ceramic Society*, **24**, 2004, p. 75
3. AMIGO, M. J., SERRANO, J.F., KOJDECKI, A.M., BASTIDA, J., ESTEVE, V., REVENTOS, M.M., MARTI, F., *Journal of the European Ceramic Society*, **25**, 2005, p. 1479
4. ECE ISIK, O., NAKAGAWA, Z., *Ceramics International* **28**, 2002, p.131
5. IQBAL, Y., LEE, E.W., *J. Am. Ceram. Soc.*, **82**, nr. 12, 1999, p. 3584
6. IQBAL, Y., LEE, E.W., *J. Am. Ceram. Soc.*, **83**, nr. 12, 2000, p. 3121
7. BRAGANÇA, S.R., BERGMAN, C.P., *Ceramics International* **29**, 2003, p. 801
8. GOREA, M., KRISTALY, F., POP, D., *Acta Mineralogica-Petrographica* **46**, 2005, in press

Manuscript received: 26.10.2006